PERGAMON

Journal of Structural Geology 25 (2003) 371–388

JOURNAL OF STRUCTURAL GEOLOGY

www.elsevier.com/locate/jsg

Structural style of the offscraped Ligurian oceanic sequences of the Northern Apennines: new hypothesis concerning the development of mélange block-in-matrix fabric

Giuseppe Bettelli, Paola Vannucchi*

Dipartimento di Scienze della Terra, Università di Modena e Reggio Emilia, Largo S. Eufemia, 19, 41100 Modena, Italy

Received 30 January 2001; received in revised form 21 January 2002; accepted 8 February 2002

Abstract

Shaly dismembered formations crop out extensively on the eastern side of the Northern Apennines, as overthrusted Cretaceous oceanic units. The lack of metamorphism and the unconformably overlain epi-Ligurian sequence, which represents the trench/slope-basin sedimentary sequence, suggest that these units are accreted sequences accomplished by offscraping and imbrication. These units are characterized by stratal disruption, lack of internal coherence and complete destruction of the original stratigraphic sequence. Block-in-matrix fabric results in symmetric boudins and systematic presence of isolated or intrafolial hinges of isoclinal folds. Two orthogonal sets of tight-to-isoclinal folds are always recognizable, involving the break-up and the boudinage of the competent layers, now transposed parallel to the axial planes of the disrupted isoclinal folds. The superposition of two generations of orthogonal tight-to-isoclinal folds may be locally observed either in single bed fragments or in some preserved coherent units. Disruption and block-in-matrix fabric is a consequence of polyphase folding and intense shortening. This geometry and kinematic interpretation well constrain the tectonic environment where these rocks were deformed to the proximity of the prism toe and within the prism itself. Thus, the Apennine broken formations result from the disruption of a sedimentary pile lying on the subducting plate of the Cretaceous to Eocene trench fore-arc system, which generated the Ligurian accretionary wedge.

Keywords: Broken formations; Tectonic mélanges; Polyphase folding; Veins; Ligurian Units; Northern Apennines

1. Introduction

Stratal disruption, block-in-matrix fabric and tectonic layering, caused by the preferred orientation of competent blocks, are the typical characters of chaotic rocks commonly known as mélanges (Hsü, 1968; Raymond, 1984; Cowan, 1985). Basic studies have distinguished three types of mélanges: sedimentary mélanges (i.e. olistostromes and the other products of mass wasting), tectonic mélanges and diapiric mélanges (Byrne, 1984; Raymond, 1984; Vollmer and Bosworth, 1984; Cowan, 1985; Kimura and Mukai, 1991). While a diapir has a typical isotropic disaggregation texture (Orange, 1990; Lewis and Byrne, 1996), the block-in-matrix fabric characterizing the sedimentary and tectonic mélanges can be the result either of the intimate mixing of blocks and mud, due to mud-flow and debris-flow processes, or of layer-parallel extension and/or shearing, due to gravitational sliding or tectonic deformation (Cowan, 1985; Brandon, 1989; Charvet and Ogawa, 1994; Hashimoto and Kimura, 1999). Among them debris-flow and mud flow deposits are easily recognizable on the basis of their fabric (Bettelli and Panini, 1989, 1992; Castellarin and Pini, 1989; Pini, 1992, 1999; Bettelli et al., 1996). Layer-parallel shearing, caused by the slicing under an overriding plate, and an extensional fabric, because of the loading, occur in sediments scraped off from a descending plate (Fisher and Byrne, 1987; Hashimoto and Kimura, 1999). These underthrusted sediments, decoupled by the overriding accretionary prism, by-pass the intense layer-parallel shortening that occurs in the offscraped units, as imaged by the present-day accretionary wedges and collisional orogens (Maltman et al., 1993; Clennell and Maltman, 1995; Maltman, 1995; Harris et al., 1998; Fruehn et al., 1999). For this reason the layer-parallel extension found in ancient offscraped units has been interpreted as superficial gravitational sliding on the inner trench-slope (Cowan, 1985).

The mélanges described in this paper make up a large part

* Corresponding author. Tel.: +39-059-205-5863; fax: +39-059-205-5887.

E-mail addresses: paolav@geo.unifi.it (P. Vannucchi), epitrepo@unimo.it (G. Bettelli).

0191-8141/03/$ - see front matter © 2002 Elsevier Science Ltd. All rights reserved.
PII: S0191-8141(02)00026-3

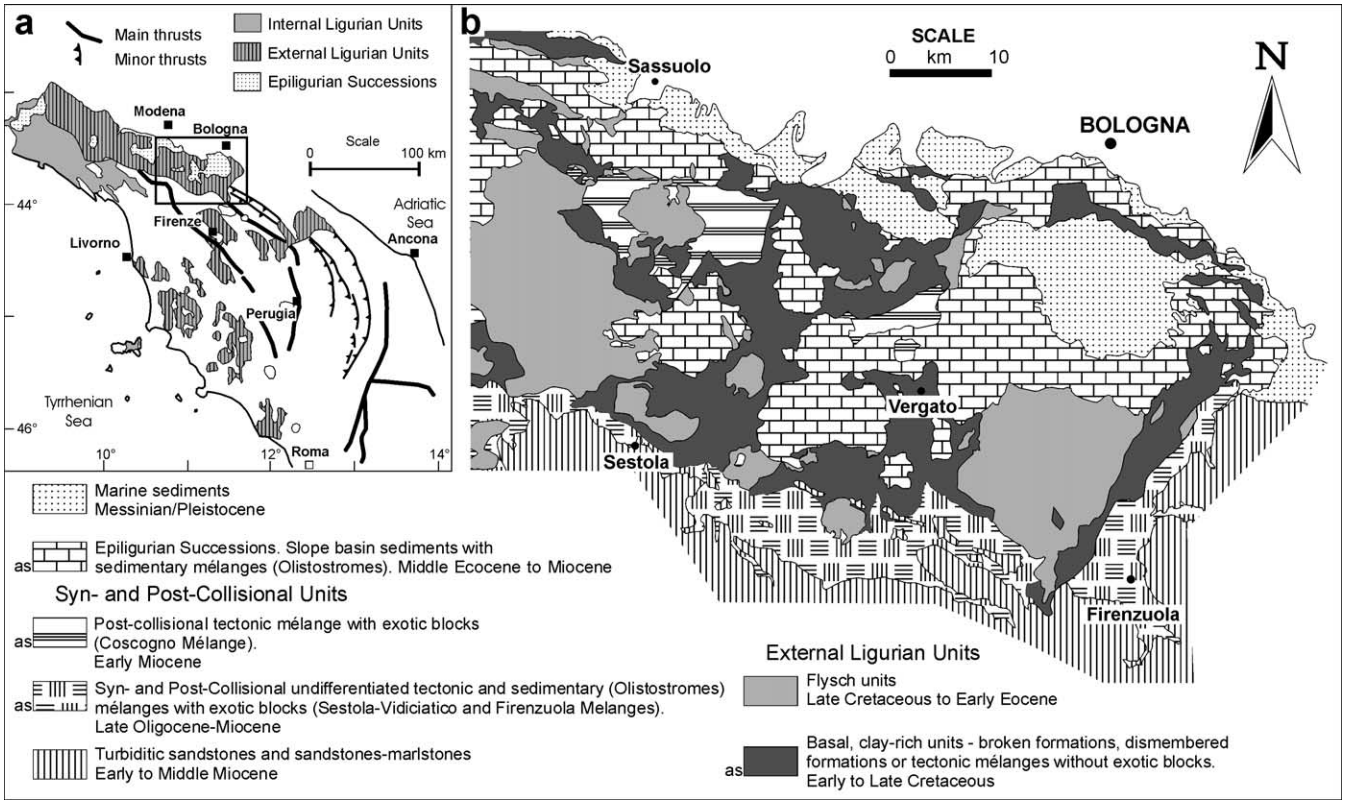

Fig. 1. (a) Tectonic sketch map showing the Ligurian Units extension in the Northern Apennines, inset shows location of (b). (b) Geologic map of the Bologna and Modena foothills. The units with 'as' in the legend were known and mapped as 'Argille Scagliose'.

of the Ligurian thrust-nappe of the Northern Apennines, tectonically disrupted in a trench-forearc environment, as unanimously recognized (e.g. Reutter, 1981; Principi and Treves, 1984; Pini, 1999). A big effort has been made, in fact, to differentiate the products of sedimentary and tectonic processes in the Apennines, while here we will concentrate on the causes of the widespread stratal disruption of these broken formations. The internal geometry of these tectonic mélanges implies a new hypothesis about their generation involving polyphase folding as a result of frontal accretion.

2. Geological framework of the Northern Apennines and Ligurian Units

The Northern Apennines is characterized by a fold-and-thrust geometry produced after the closure of the Ligure–Piemontese ocean basin and the collision of the Adria and European continental blocks starting from the Oligocene (Boccaletti et al., 1980; Reutter, 1981; Treves, 1984; Coward and Dietrich, 1989; Deiana and Pialli, 1994; Marroni and Treves, 1998). The pre-collision phase of convergence, either related to an Eoalpine (Vai and Castellarin, 1993; Pini, 1999; Vescovi et al., 1999), or to an early Apennine (Reutter, 1981; Principi and Treves, 1984; Treves, 1984) tectonic phase, caused the deformation of the Ligurian Units and the development of a Late Cretaceous–Middle Eocene accretionary wedge. The Ligurian accretionary wedge is emplaced, as a thrust-nappe, on top of the Apennine pile and is unconformably overlain by a trench-slope basin sequence, epi-Ligurian, of Middle Eocene–Late Miocene age (Ricci Lucchi, 1987; Bettelli et al., 1989b).

The Ligurian thrust-nappe is characterized by several stratigraphic sequences and/or tectonic units, each one representing a different paleogeographic domain of the former Ligure–Piemontese oceanic basin. The main partition is between the Internal and the External Ligurian Units, two large groups of sequences and tectonic units separated by a high angle fault of unclear kinematic significance (Marroni and Treves, 1998) (Fig. 1). The Internal Ligurian Units are coherent and slightly metamorphic and still have remnants of an ocean floor basement consisting of ophiolites with their sedimentary cover (Fig. 1) (Abbate and Sagri, 1970; Marroni and Pandolfi, 1996), formed by a clay-rich basal sequence and a thick turbiditic, "flysch" sequence, on top. They have been recently interpreted as underplated units (Marroni, 1994).

The External Ligurian Units (Fig. 1) are not metamorphosed and their clay-rich basal sequence is incoherent and characterized by widespread internal stratal disruption. In spite of the incoherent basal sequence the overlying thick pile (up to a few thousand meters) of Late Cretaceous to

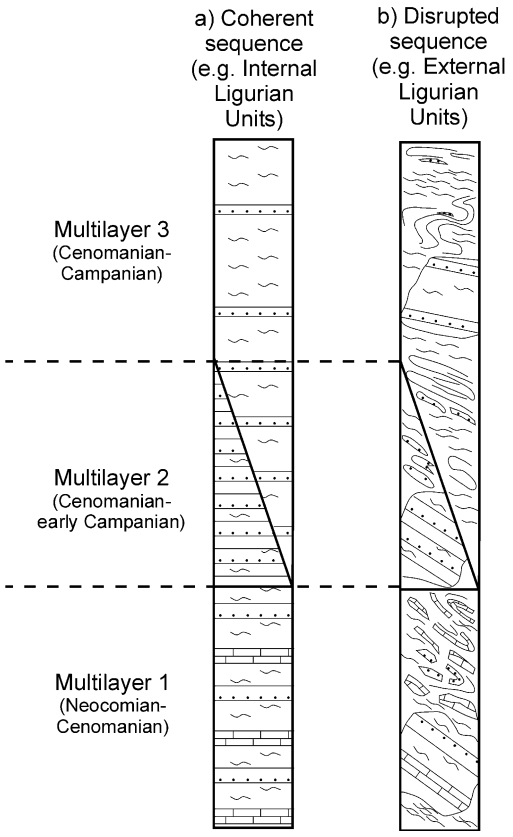

Fig. 2. Schematic columns showing the basal portion of the Ligurian Units either as coherent (a), where the contacts among multilayers are stratigraphic, and as disrupted sequence (b), where the contacts among multilayers have been tectonized, even though the multilayers maintain the original geometric position one to another.

Early Tertiary calcareous and/or arenaceous turbidites (Helminthoid Flysch) are still coherent. These turbidites represent the infilling of a deep-sea trench basin and/or sedimentation on the Tethyan oceanic plate and they are deformed by regular, map-scale folds. The unconformably overlying epi-Ligurian sequence suggests that disruption took place at a shallow structural level.

Until the 1970s, the incoherent basal sequence of the External Ligurian Units was grouped with other chaotic rocks under the comprehensive general term of 'argille scagliose' (i.e. argille scagliose–scaly clays or scaly shales: Merla, 1952; Page, 1963) (Fig. 1b) or 'Chaotic Complex' (Abbate and Sagri, 1970). In the past two decades, new detailed structural and stratigraphic studies (Bettelli and Panini, 1989, 1992; Bettelli et al., 1989a, 1996; De Nardo, 1994; Pini, 1999 and references therein) have led to the distinction among the different stratigraphic and/or tectonic units forming the argille scagliose. In particular, a clear distinction has been made between sedimentary mélanges (i.e. olistostromes—most of which are intercalated in the epi-Ligurian sequence and in the syn- and post-collisional Oligocene–Miocene foredeep turbidite sequences of Fig. 1b—and huge gravitationally displaced masses: e.g.Val Rossenna sequence mélange: Bettelli and Panini, 1989), mélanges of uncertain origin with exotic blocks (e.g. Firenzuola mélange and Sestola–Vidiciatico tectonic unit; Fig. 1b; Bettelli and Panini, 1989, 1992), tectonic mélanges with exotic blocks (e.g. Coscogno mélange; Fig. 1b; Bettelli and Panini, 1989), and finally broken or dismembered formations (Bettelli et al., 1989a; Bettelli and Panini, 1989, 1992; Pini, 1999). Their distinction leads also to their identification as very different products of sedimentary/tectonic processes, accompanying the building-up of the Apennine chain, from oceanic accretion to collision.

The incoherent basal portion of the External Ligurian Units (Fig. 1b) has been recognized as tectonically disrupted for many years (Pini, 1999 and references therein), based on:

- The age of deformation. The time upper limit for disruption is the collision between the European and Adria plates, i.e. Middle Eocene (Bettelli and Panini, 1989). The disruption, in fact, occurred in a compressional tectonic environment characterized by the growth of an accretionary prism (Reutter, 1981; Principi and Treves, 1984), as testified by large (up to 100 km wide and 700–800 m thick) slided masses and thick chaotic sedimentary deposits (olistostromes) lying on top of the Ligurian Flysch sequence (as in the case of the Val Rossenna sequence: Bettelli and Panini, 1989), of the tectonic mélanges (or broken/dismembered formations), or at the base of the epi-Ligurian sequence (Bettelli and Panini, 1989; Pini, 1999). The conformity between the basal sequence and the overlying flysch gives a time lower limit implying that the disruption occurred after Late Cretaceous–Eocene. Discontinuities within the basal sequence, proposed only on the basis of the stratigraphic, not deformational, record, have to be related to early compressional events controlling the Ligurian oceanic basin (e.g. Vescovi et al., 1999; Pini, 1999). Compression and subduction, in fact, were active since the Late Cretaceous as demonstrated by the chemical features of ophiolitic metabasalts occurring as dispersed blocks in the basal sequence of the External Ligurian Units (Capedri and Toscani, 2000) and the transpression affecting the flysch deposition (Marroni and Treves, 1998).
- In contrast to the disruption of the basal sequence, the overlying Late Cretaceous to Tertiary Ligurian flysch sequence crops out as large, coherent and mildly deformed slabs with map-scale folds, mainly consisting of large overturned synclines. This style of deformation testifies to layer-parallel shortening due to tectonic compression related to the Ligurian ocean closure.
- Sedimentary processes such as debris flow and mud flow produce clasts dispersed in a real, detrital matrix, through disaggregation and new deposition, while tectonic stress and mass movement by gravitation induces disruption

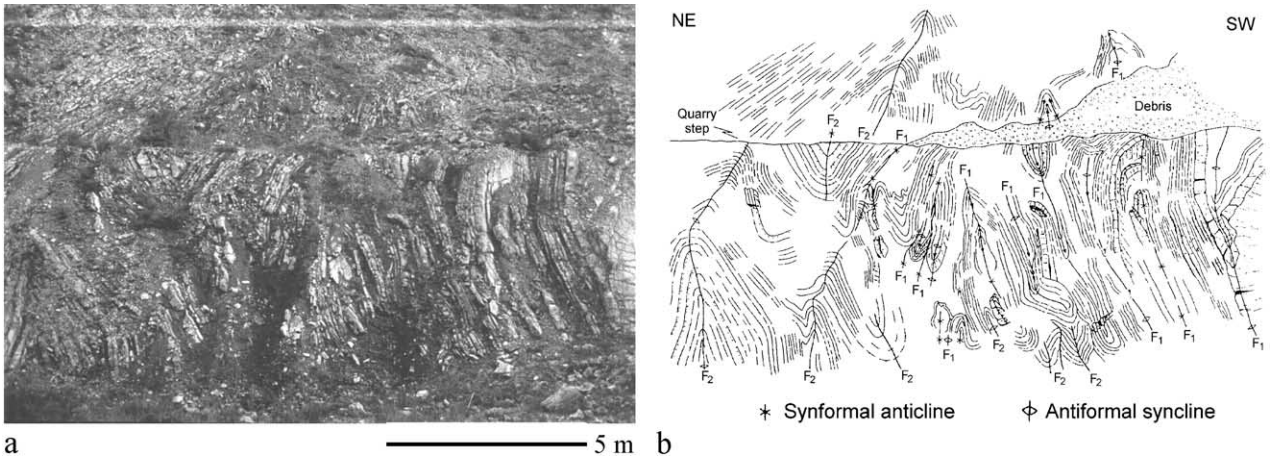

Fig. 3. Photograph (a) and sketch (b) of coherent Multilayer 1 outcrop showing two perpendicular folding phases: F_1 and F_2 are the axial plane/topography intersection of, respectively, the first and second folding phases (modified from Bettelli et al., 1996).

through a mechanism of layer-parallel extension or layer-parallel shortening where blocks are eventually dispersed in a rheological weak unit (Byrne and Fisher, 1990; Orange, 1990; Kusky et al. 1997; Kusky and Bradley, 1999). This basic difference combined with a careful analysis of the structural and stratigraphic context in which they are found allowed the distinction of tectonic, sedimentary and sedimentary–tectonically reworked mélanges in the Apennines (Bettelli et al., 1989a; Bettelli and Panini, 1989, 1992; Pini, 1999).

- The deformation structures in the Ligurian mélanges appear to have been developed during different stages of lithification, according to a progressive tectonic event occurring gradually at a rate comparable with diagenesis. Gravitational events, on the contrary, are short and episodic so that they punctuate the diagenetic history (Maltman, 1995).

3. The clay-rich, basal sequence of the External Ligurian Units

All the basal clay-rich sequences of the External Ligurian Units and of the sedimentary portion of the Internal Ligurian Units have similar lithologies and a distinctive ratio between the thickness of the competent and incompetent layers. Thus, apart from the different lithostratigraphic subdivisions recently introduced by the Italian geologists, each sequence can be described as composed by three different multilayers (Fig. 2) reflecting three main depositional environments. From the bottom to the top:

- MULTILAYER 1: layered sequence of alternating gray to black shales and fine-grained calcareous or siliciclastic turbidites of varying thickness (basin plain deposit, Lower Cretaceous, i.e. Argille a Palombini, auctt.) (Fig. 3a);
- MULTILAYER 2: fine grained turbidite sandstones alternated with gray shales, locally marlstones, with a rather variable layer thickness and sandstone/shale ratio (deep water submarine fan deposit, Cenomanian to Early Campanian, i.e. Arenarie di Ostia, Arenarie di Scabiazza, auctt.);
- MULTILAYER 3: thin bedded shales of different colors (red, gray, green, black, etc.) with sparse beds of turbidite sandstones, marlstones and limestones (abyssal plain deposit, Cenomanian to Campanian, i.e. Argille Varicolori, auctt.).

On the outcrop scale the described multilayers of the External Ligurian Units show a ‘block-in-matrix’ fabric apparently derived from layer-parallel extension of the original sequences, as well as a striking tectonic layering produced by sub-parallel alignment of competent inclusions, by the scaly fabric affecting the shales and, locally, by the preserved primary bedding (Fig. 2). Thus they retain neither primary contacts within the sequence nor the original stratigraphic relationships. Nevertheless these multilayers maintain a geometric position which correspond to their stratigraphic location in the coherent successions of the Internal Ligurian Units (Fig. 2).

Despite the general stratigraphic disruption, coherent units are locally preserved as large bodies providing information both on the primary sedimentary characteristics and on the different stages of deformation (Fig. 2). As a rule these multilayers are coherent if the shaly, weak beds are thinner than the strong beds.

The minor structures associated with the Ligurian mélanges include folds, boudinage and pinch-and-swell, scaly foliation and veins. Such a disrupted sedimentary sequence is described through the continuous comparison with the preserved bodies of coherent multilayer, where different stages of progressive deformation/disruption are visible.

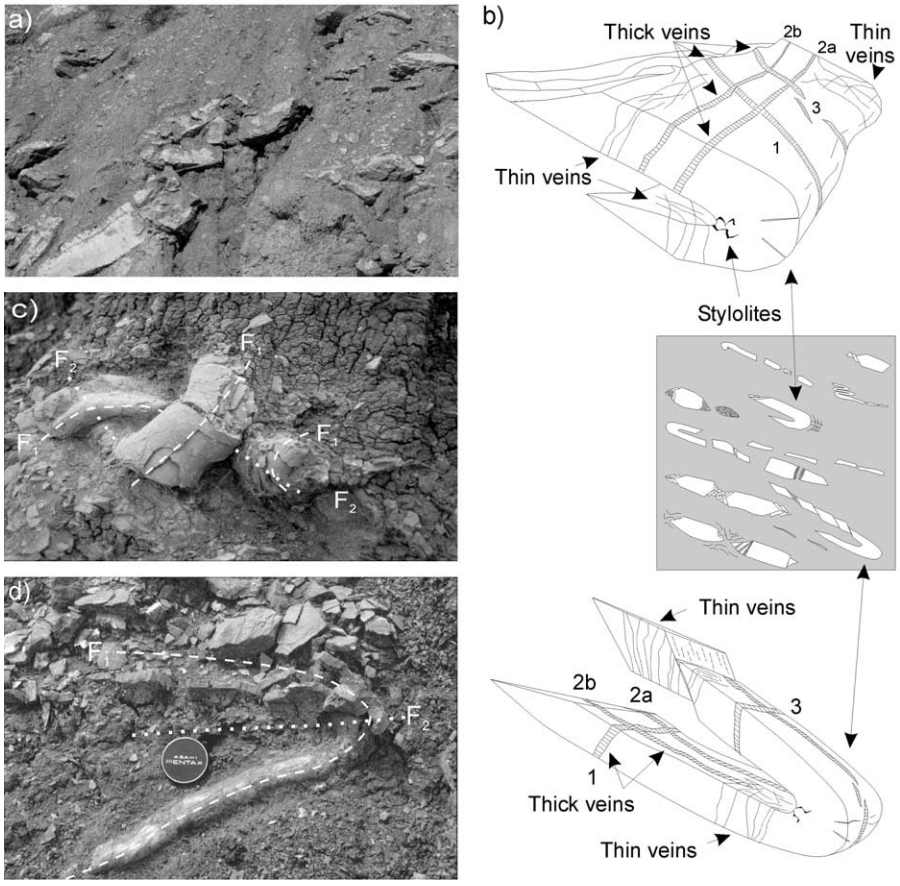

Fig. 4. (a) Disrupted Multilayer 1. (b) Schematic summary of principal mesoscopic structures in the disrupted Multilayer 1: unpatterned areas represent limestone layers with a matrix of scaly clay (shaded), with close-up of folds showing internal features. (c) and (d) Examples of interference between the two perpendicular folding phases F_1 (dashed) and F_2 (dotted) recognized in the disrupted Multilayer 1. The strong non-cylindrical character of F_1 is evident on the left side of the photo (c).

4. Multilayer 1

4.1. Structural style of alternating shales and limestones

Multilayer 1, as a rule, crops out disrupted and characterized by a block-in-matrix style of deformation (Fig. 4a). The rare coherent portions always have limestone beds systematically thicker than shale interbeds. The shales are characterized by a well developed fissility parallel to the bedding (Fig. 5a). In the disrupted Multilayer 1 the rheologically strong limestone beds occur as blocks dispersed within the shales working out as a weak unit (Fig. 4a and b). In three dimensions, the limestone blocks are either elongated or roughly equidimensional with shapes from prismatic–rectangular to lenticular. Each block displays well preserved primary sedimentary structures, i.e. grading, parallel and/or oblique lamination, flute and groove casts or trace fossils. These structures are useful for determining the stratigraphic way-up of each block. Block alignment closely resembles bedding, as it contains sedimentary structures and the interfaces between layers may be original, nevertheless this layering is a product of transposition where folding processes generate reorientation of the bedding into an orientation approximately parallel to the axial plane of the folds (folding transposition) (Fig. 5a and b). Thus, the blocks statistically define a pronounced tectonic layering concordant with a penetrative mesoscopic foliation and the scaly fabric developed in the clay. The preferred orientation of blocks defines a planar mesoscopic structure persistent at the scale of the map that tends to be parallel to the contact of the other multilayers.

4.1.1. Boudinage and pinch-and-swell structures

Blocks exhibiting squared terminations and rectangular cross-sections are controlled by Mode II and Mode III shear fractures or by Mode I extensional fractures, lying, respectively, at high angle or perpendicular to S_0 (Fig. 4b). On the block termination, slickenlines, fibrous calcite steps and calcite veins, both of extensional and shear type, further suggest the detachment mode.

Accessory features help to show how the lenticular blocks achieved their final shape. They may show, for example, elongated and thinned terminations accommodated by a cemented breccia. Commonly single breccia fragments are displaced and rotated. Cataclasis can affect the whole block or, more commonly, their terminations, already defined by

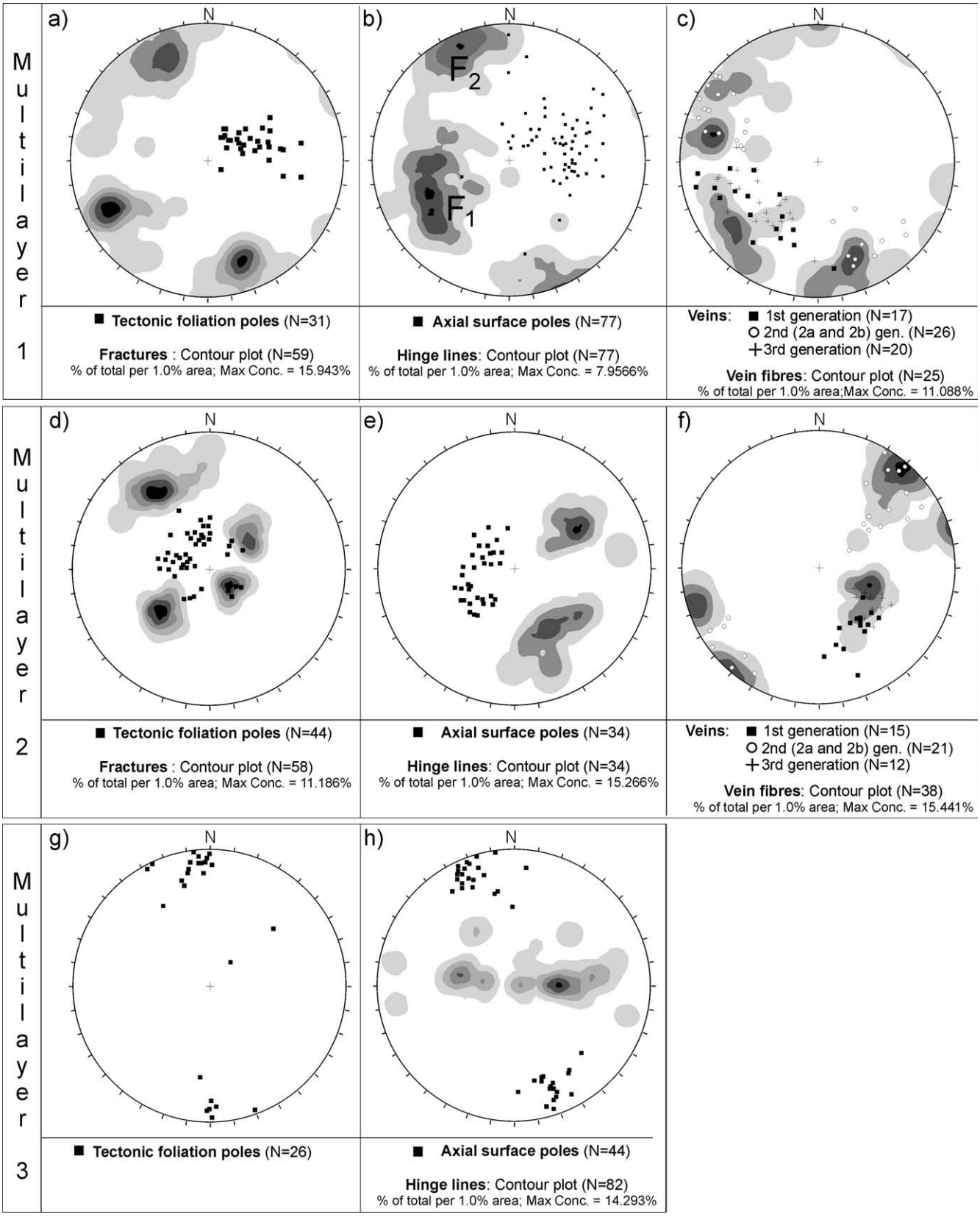

Fig. 5. Pole and contoured stereograms, lower hemisphere, from the three multilayers.

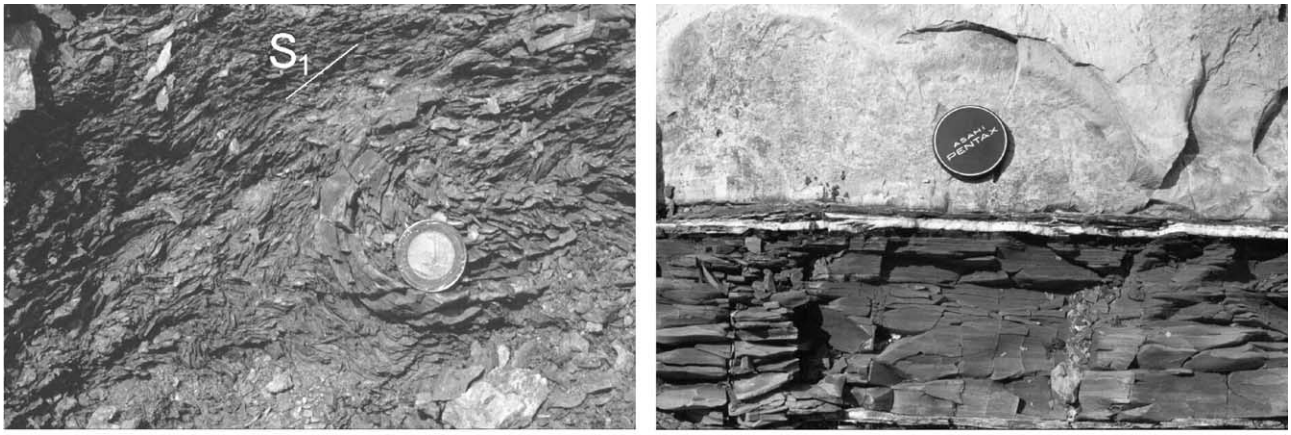

Fig. 6. (a) Fold hinge in the shaly sediment: the axial plane cleavage is parallel to the tectonic layering and to the scaly fabric defining the S_1 foliation. (b) Fibrous extensional calcite veins formed at the competent/incompetent interface.

the intersection between extensional or shear fractures and S_0. Lenticular terminations may also be formed either by the intersection of two or more conjugate extensional shear fractures or by a single extensional shear fracture defining an asymmetrical wedge, whose translation or rigid rotation accomplish the final shape of the block. Thus, while the squared terminations preserve the geometry of the original surface of separation, the lenticular shape is achieved by breaking or translating already formed blocks. On the other side, folded shales characterize the block's neck region. These folds indicate flowing of unlithified material to fill the gap created by the separation of the blocks. The flow induces further stress on the block edges giving modifications to the lenticular shapes.

The bedding surfaces of the limestone blocks exhibit grooves, mechanical striations or, more rarely, thin overgrowths of fibrous calcite steps. Locally these features define two overlapping generations of mechanical lineations intersecting each other at high angle.

4.1.2. Folds

In the incoherent units the limestone blocks are often formed by isolated hinges of close to isoclinal folds as well as by intrafolial fold hooks. Looking at the coherent units, they show a complex internal geometry with two or three different generations of mesoscopic folds (Fig. 3a and b). Starting from the analysis of coherent units, the older folds, F_1, are metric in size, typically non-cylindrical and show close to isoclinal interlimb angles. The folds in the limestone layers vary from parallel to class 1C, while in the shales they belong to class 3 or 2 (sensu: Ramsay and Huber, 1987). The shales in the fold limbs show either a very strong fissility or a penetrative and anastomosing foliation, both of them parallel to the tectonic layering and to S_0 (Fig. 6a). Scaly fabric develops to accommodate either the differential slip among competent and soft layers or the limb thinning. The shaly interbeds are also affected by an axial plane cleavage, parallel to the tectonic layering and to the scaly fabric (Fig. 6a). All the described elements define the S_1 foliation. The axial plane cleavage intersects the fissility and produces a typical pencil cleavage with L_1 lineation lying parallel to the fold hinge lines. The limestone layers do not develop axial plane cleavage, they instead have joints, extensional–contractional fractures or rare stylolites concentrated in the hinge outer and inner arc. Hinge lines of these non-cylindrical folds have culminations and depressions. F_1 hinge lines are dipping toward SW (Fig. 5b), but after the geometric restoration obtained by subtracting later folding events, F_1 folds are isoclinal recumbent folds verging at 90° to the NE Apennine mean vergence direction.

The second folding phase, F_2, detected in coherent portions of Multilayer 1, produced folds with the same characters as F_1, except for the disharmonic style developed as a consequence of refolding the sequence. F_2 have developed perpendicular to F_1 (Figs. 3a and b and 4). They have hinge lines oriented NW–SE and verging NE (Fig. 5b), in accordance with the Apennine setting. F_2 usually developed bigger folds than F_1, with a curvature radius in the order of tens of meters. Thus the interference pattern between F_1 and F_2 is difficult to observe, even though it resembles type 2 of Ramsay and Huber (1987). F_1–F_2 interference is expressed locally by the pencil cleavage orientation, sometimes lying at high angle, sub-perpendicular to the fold hinge lines. The other effect of F_1–F_2 interference is to produce folds often represented by antiformal synclines and synformal anticlines.

F_3 folds are open and recumbent and have a NE vergence. F_2 and F_3 are coaxial, and the latter may well be a further evolution of F_2, rather than a new folding phase. F_3 has been observed only in few coherent outcrops of Multilayer 1. In the incoherent units the hinge lines of the isolated and rootless folds are, in fact, statistically arranged around two preferential directions, mutually at high angles or perpendicular, exactly like F_1 and F_2.

In the completely disrupted units folding phases are difficult to recognize. In fact F_1 and F_2 axial planes and

the tectonic layering are parallel. Considering the tectonic layering as a geometrical frame, F_2 hinge lines are coincident with the tectonic layering strike, whereas F_1 hinge lines are parallel to its dip direction. The dispersion around these two principal orientations is quite high, going from 20° to 30° as calculated through the stereographic projections (Fig. 5b), but the disrupted nature of the outcrops brings an error in the plots, since the data are collected areally, and the non-cylindrical character of the folds is enhanced in the disrupted volumes. The lack of cylindricity is more visible in the sandstone than in other blocks, because of the poor lithification of the siliciclastic component. Single blocks showing the two systems of superimposed decimetric folds are frequent (Fig. 4c and d). The perpendicular hinge lines form type 2 interference patterns (Ramsay and Huber, 1987). The sedimentary structures show upright and overturned blocks resting along the tectonic layering, helping in the identification of folded sequences.

Some common characters of the folds help in defining the mechanisms and physical properties of the Multilayer 1 during deformation, e.g. the shapes of the folds, the scaly fabric location and the axial plane cleavage absence. Folded shales usually show a strong limb thinning, whereas the limestone layers, deformed when they were already lithified, behave as a strong rheological component. On the other hand the shales in the F_1 hinges do not show scaliness. Scaly fabric is the effect of the limb concentration of shear strain in the shaly, incompetent interbeds during the folding mechanism. The absence of axial plane cleavage in the strong layers further demonstrates that the folding took place at shallow structural levels.

4.1.3. Veins

Shale and limestone are both cut by intense veining. Shales have veins parallel to the tectonic foliation and to the transposed S_0 that never propagate across the limestones. These are fibrous calcite veins of extensional type and, as observable in coherent sequences of Multilayer 2, they preferably form in the higher portion of the pelitic layer or at the shale/limestone interface (Fig. 6b). Isoclinal folds clearly deform these veins. Calcite veins in the limestone may be distinguished in two different types based on their dimensions and geometric characteristics (Fig. 4b): thin veins, ranging from sub-millimeter to some millimeters in thickness, and thick veins, ranging from few millimeters to some centimeters in thickness. In the first case the calcite fabric cannot be determined in the field, but only in thin section, while in the second case it is always possible to distinguish the fibrous or blocky calcite. The thin veins form an anastomosing network preferentially arranged at high angles to the tectonic layering. They have either strike variability or variable dip angles. Besides the anastomosing geometry, the thin veins may change their relative thickness as easily observable in cross-section perpendicular to the tectonic layering. The thin veins are the older structure observed within the limestone blocks since they are cut both by the thick veins and extensional shear fracture systems. Thin veins are also always folded by the two folding systems.

The thick veins are tabular and filled by fibrous or mosaic calcite. Cross-cutting relationships between thick veins indicate that older veins are always characterized by fibrous calcite, while younger veins have either fibrous or mosaic textures. These calcite veins lie in two preferential directions at a high angle to each other and perpendicular to tectonic layering (Fig. 5c), so that they produce a characteristic chocolate tablet appearance as seen in the plane of the tectonic layering.

Generally the calcite fibers are perpendicular, or sub-perpendicular, to the fracture walls and they are always parallel or sub-parallel to the tectonic layering (Fig. 5c). Further development of the calcite fibers maintains a constant angle to the vein walls. Systematic measurements of calcite fiber orientations show that they follow two preferred orientations, corresponding to the hinge lines of the two sets of isolated folds (Fig. 5c). Systematic cross-cutting relationships between the two orientations have been observed. The oldest veins are perpendicular to the F_1 hinge line and folded by it (vein 1 in Fig. 4b). The oldest veins are then cut by a second vein set parallel to F_1 and perpendicular to F_2 hinge line (vein 2 in Fig. 4b). Finally the youngest set of veins resembles the situation of the oldest set (vein 3 in Fig. 4b). Considering F_1 and F_2 we can infer, looking for symmetry, that each folding phase is related to one vein system, each one composed of one vein set perpendicular and the other parallel to the correspondent hinge line (Fig. 4b). For this reason vein 2 in Fig. 4b is either attributed to the F_1 vein system, as vein 2a, or to the F_2 vein system, as vein 2b. This vein web suggests that the rheologically strong component of Multilayer 1 experienced at least two extension episodes along two perpendicular directions. The calcite fibers setting implies that they initiated with a maximum incremental longitudinal strain oriented perpendicular to the bedding and that they develop with a constant principal incremental strain.

As already mentioned the orientations of calcite fibers, the vein set's geometry and the fold hinge lines of the two folding events are geometrically connected (Fig. 5a–c). In fact, each fold is associated first with the veins with the calcite fibers parallel to its hinge line and then with the veins with fibers perpendicular to the same hinge line. Considering the folding order, this geometry implies that during F_1 the extension along the tectonic layering dip direction has taken place before the extension along strike. Then during F_2 a new extension took place along strike followed by an extension along dip direction.

The presence of two non-coeval and sub-perpendicular directions of extension, along the tectonic layering dip direction and strike, is also confirmed by other brittle structures. These are shear fractures of Mode III arranged in two sub-perpendicular sets lying at high angle to the tectonic layering. These extensional shear fractures are either planar

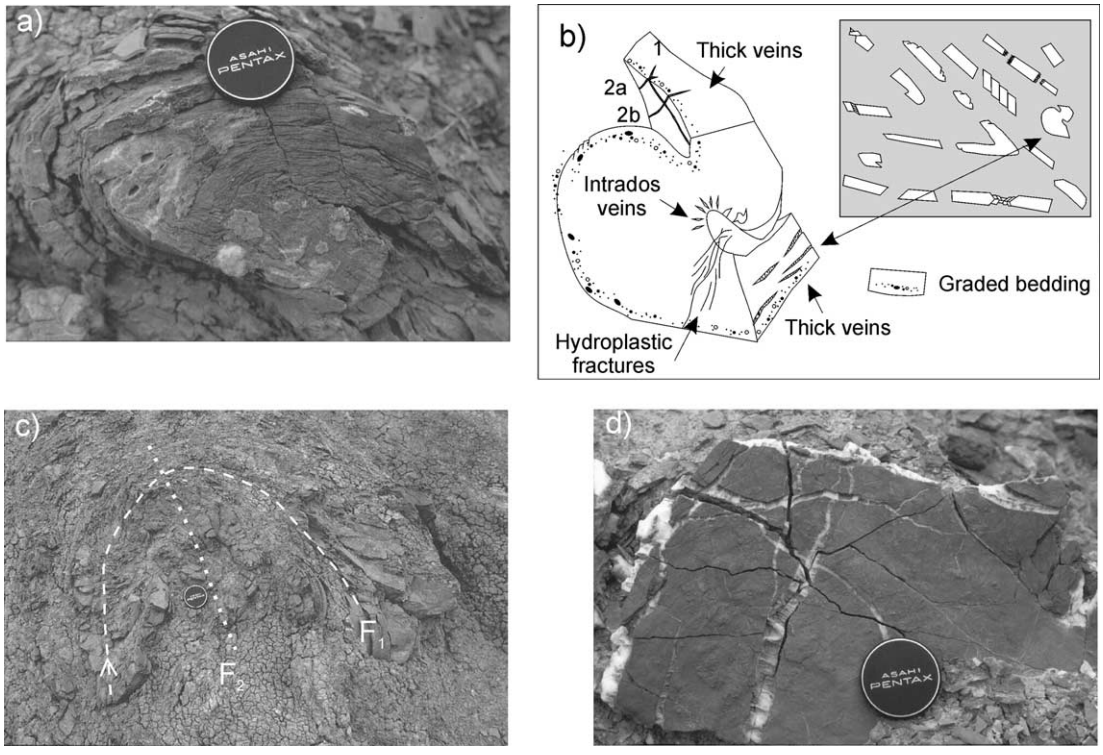

Fig. 7. (a) Fold hinge developed in a sandstone layer of the disrupted Multilayer 2. (b) Schematic summary of principal mesoscopic structures in the disrupted Multilayer 2: unpatterned areas represent sandstone layers with a matrix of scaly clay (shaded), and close-up of folds showing internal features. (c) Example of interference between the two perpendicular folding phases F_1 (dashed) and F_2 (dotted) recognized in the disrupted Multilayer 2. (d) Sandstone block bounded by extensional calcite veins cross-cutting at 90°.

or listric and they give a characteristic staircase appearance to the limestone blocks or, if they are concentrated at the block endings, they form apexes and thinned terminations (Fig. 4b). The age and geometric relationships of the extensional shear fractures with the isolated fold hinge lines are the same as showed by the calcite veins. The relationships between fold hinges, thin and thick calcite veins and extensional shear fractures are directly detectable in the field. The limestone beds, finally, show systematic joints always arranged perpendicular to S_0, with slickenlines typically parallel to the intersection between S_0 and the joint surfaces. The geometric relationships between the joint systems and their kinematic indicators argue that they are shear joints formed by compression parallel to the bedding when it was still horizontal. Cross-cutting relationships indicate that the thin calcite veins are older than the systematic shear joints, but the latter are also always refolded by the two folding systems like the thin vein sets.

5. Multilayer 2

5.1. Structural style of alternating sandstones and shales

Multilayer 2 consists of alternating fine-grained siliciclastic turbidites and pelites. The combination of characters such as the sandstone/shale ratio, the thickness of the beds and the clay percentage in the pelite horizons, allow the distinction of four different lithofacies each one corresponding to a distinct mesoscopic structural style. The four lithofacies are:

1. lithofacies 1 is represented by fine to medium-grained sandstones grading up into thin shale intervals, the sandstone beds are medium to thick (10 cm–1 m), sandstone/shale ratio > 1;
2. lithofacies 2 consists of marlstones with subordinate sandstone beds;
3. lithofacies 3 is represented by a regular alternation of sandstones and shales organized in thin to medium beds (3–10 cm), with sandstone/shale ratio $= 1$;
4. lithofacies 4 is characterized by shales with subordinate fine-grained sandstones and siltstones in layers ranging in thickness from centimeter to decimeter although scattered thicker beds may be locally present. The sandstone/shale ratio is <1. Owing to the reduced thickness of sandstone and siltstone layers, this lithofacies essentially crops out as a shaly unit not easy distinguishable from Multilayer 3.

Lithofacies 1 and 2 are not abundant and characteristically crop out as coherent, mappable units, without appreciable deformation except for systematic joints and rare extensional calcite veins. Mesoscopic folds have never

been observed. Nevertheless, these lithofacies with overturned beds crop out almost anywhere (Bettelli et al., 1989a). Reduced exposures, overturned beds and internal coherence characterize also lithofacies 3, even though mesoscopic folds are locally visible and characterized by being isolate, asymmetrical and frequently of chevron style. These folds are interpreted as minor or parasitic folds.

Lithofacies 4 is the most common and widespread, always cropping out as a shaly mass with a penetrative scaly fabric containing elongated flat blocks of fine-grained sandstones or siltstones floating in the shales (Fig. 7a and b). Lithofacies 4 displays a typical block-in-matrix fabric resembling the structural style of Multilayer 1. The single bed fragments preserve primary structures such as grading and oblique or parallel lamination, flute casts, tool casts and trace fossils. These primary structures indicate that the elongated, flat sandstone blocks represent fragments of original, single layers organized in a generally striking preferred orientation (Fig. 5d) concordant with the mesoscopic foliation and the scaly fabric of the surrounding shales. Locally the blocks are not aligned along the same planes so that the geometric relationship between them resembles a low to relatively high angle cross-stratification. This appearance is due to the disruption of close to tight, rather than isoclinal, folds. The incomplete development of a well-defined tectonic foliation in Multilayer 2 causes a greater dispersion of the fabric data than in Multilayer 1. This character locally makes it difficult to correlate different outcrops and even structures within the same outcrop.

5.1.1. Boudinage and pinch-and-swell structures

The blocks have straight or pointed terminations with the consequent variation of their shape from rectangular to lenticular. Fracture mode controls the block shaping as already described for Multilayer 1 (Fig. 5d). The non-coeval cross-cutting systems of extensional shear fractures are only visible on the lower S_0 surface or in cross-section, where they cut the bedding surfaces producing steps, but they do not have a visible physical expression within the sandstone layer. In other words the fracture displacements are well developed as steps on the lower surface of the sandstone turbidite beds, but they vanish inside the bed. In polished sections the shear fractures appear as cohesive micro-faults deforming the turbiditic Tc and Td intervals through drag micro-folds. Microscopic observations on the micro-faults show that they do not break the detrital grains, but they follow their boundary surfaces, at places rotating them. This ductile style of deformation by grain-boundary sliding implies that the hydroplastic shear fractures have been formed when the sandstone beds were still uncemented, or that the shear deformation took place when the diagenesis was not yet complete. Evidence of pre-lithification deformation is absent in the carbonate-rich competent layers of the Multilayer 1, even though the rare thin turbidite siliciclastic beds show the same structural features as in Multilayer 2. This suggests that in Multilayer 1 deformation took place when carbonate layers were already lithified whereas the siliciclastic layers were still unlithified.

5.1.2. Folds

Close to isoclinal folds, usually of chevron style are scattered throughout Multilayer 2 outcrops. Folds are not usually visible in Multilayer 2, even though the presence of both upright and overturned bed fragments in the same outcrop, characterized by the same tectonic layering, implies the common presence of these features. Very common instead are isolated fold closures or fold hooks, rootless folds or fold trains (Fig. 7a), usually having the same chevron style. In the highly disrupted units fold axial surfaces are typically parallel to the tectonic layering and the hinge lines statistically correspond to the foliation strike and dip direction (Fig. 5e).

Fold hinges show a whole series of deformation styles. Some isolated fold hinges do not show deformation either in the extrados or in the intrados (Fig. 7). The extension and shortening, in the outer and inner arcs of the folds, respectively, were accommodated at the grain scale without apparent loss of cohesion. Common features are veins both in the outer and inner arcs of the folds (Fig. 7b), where shortening should be concentrated. Only at the microscale anastomosing seams surrounding the sandstone grains with no breakage and at places rotating them reveal the deformation. The lack of metamorphism indicates that such conditions were possible only if the detrital grains were free to move because of the absence of lithification. The inferred mechanism of deformation is frictional grain-boundary sliding. The lack of lithification is inferred also from the intrados veins, which are compatible with the squeezing of fluid-rich sediment during folding. The ductile style of deformation is the striking characteristic of Multilayer 2, differentiating it from Multilayer 1. Here the deformation during lithification generates ductile folding style near fold hinges with axial plane cleavage and purely brittle fractures. The deformation occurred as hydroplastic shearing following the folding mechanism.

The geometrical analysis of the coherent and disrupted Multilayer 2 reveals the presence of two, superposed folding events. F_1 and F_2 have the same characters as described for Multilayer 1 (Fig. 5e). Interference patterns of the two superposed folding events are common (Fig. 7c). F_3, coaxial to F_2, is also present, even though less visible due to scaling and geometrical relationship in the disrupted units.

5.1.3. Veins

In the shales calcite veins are parallel to the tectonic layering, as observed in Multilayer 1 (Fig. 6b). The veins in the sandstone are similar to those in Multilayer 1, except for the lack of thin veins. Veins are filled by fibrous calcite, with fibers parallel to S_0, arranged in two non-coeval systems cross-cutting each other at a high angle (Figs. 5f and 7d). The veins indicate two directions of extension, active at different times and affecting the sandstone blocks

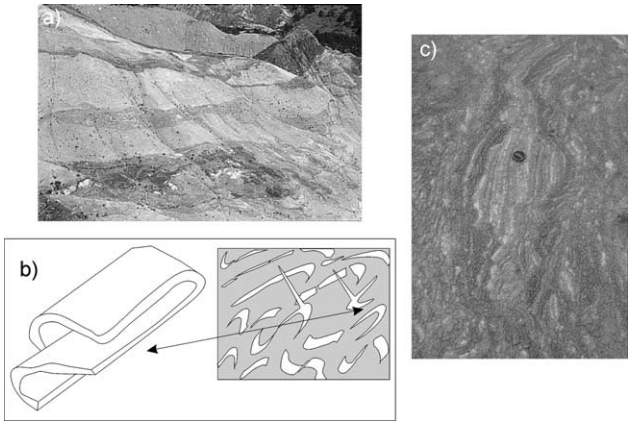

Fig. 8. (a) Disrupted Multilayer 3. (b) Schematic summary of principal mesoscopic structures in the disrupted Multilayer 3: both unpatterned and shaded areas are scaly clay. The close-up of fold shows the 3D shape of interference pattern. (c) Boudin.

(Figs. 5f and 7d). The fibrous veins are cut by later blocky calcite veins and extensional shear fractures arranged in two conjugate systems at high angle to S_0. The two perpendicular systems indicate two non-coeval directions of extension parallel both to the foliation surface and to the bedding. The cross-cutting relationships of the shear fractures suggest an evolution similar to that of the vein systems described for Multilayer 1.

6. Multilayer 3

6.1. Structural style of alternating shales with sparse turbidite sandstones, marlstones and limestones

The structural style of Multilayer 3 is the most complex of those examined. The few competent layers do not act as a frame of reference as in the other cases because of their paucity and of the different style of deformation due to the very high competence contrast. Therefore the comparison between coherent and incoherent multilayers is still particularly helpful.

The coherent portions of Multilayer 3 are characterized by an alternation of thin to medium (6–8 cm) shaly layers of different colors: red, green, black, light gray. In the incoherent portions primary bedding is no more recognizable and the shaly beds are laterally discontinuous lacking any stratigraphic order (Fig. 8a and b). Regular and sub-planar shear surfaces, a meter to several meters long, intersecting each

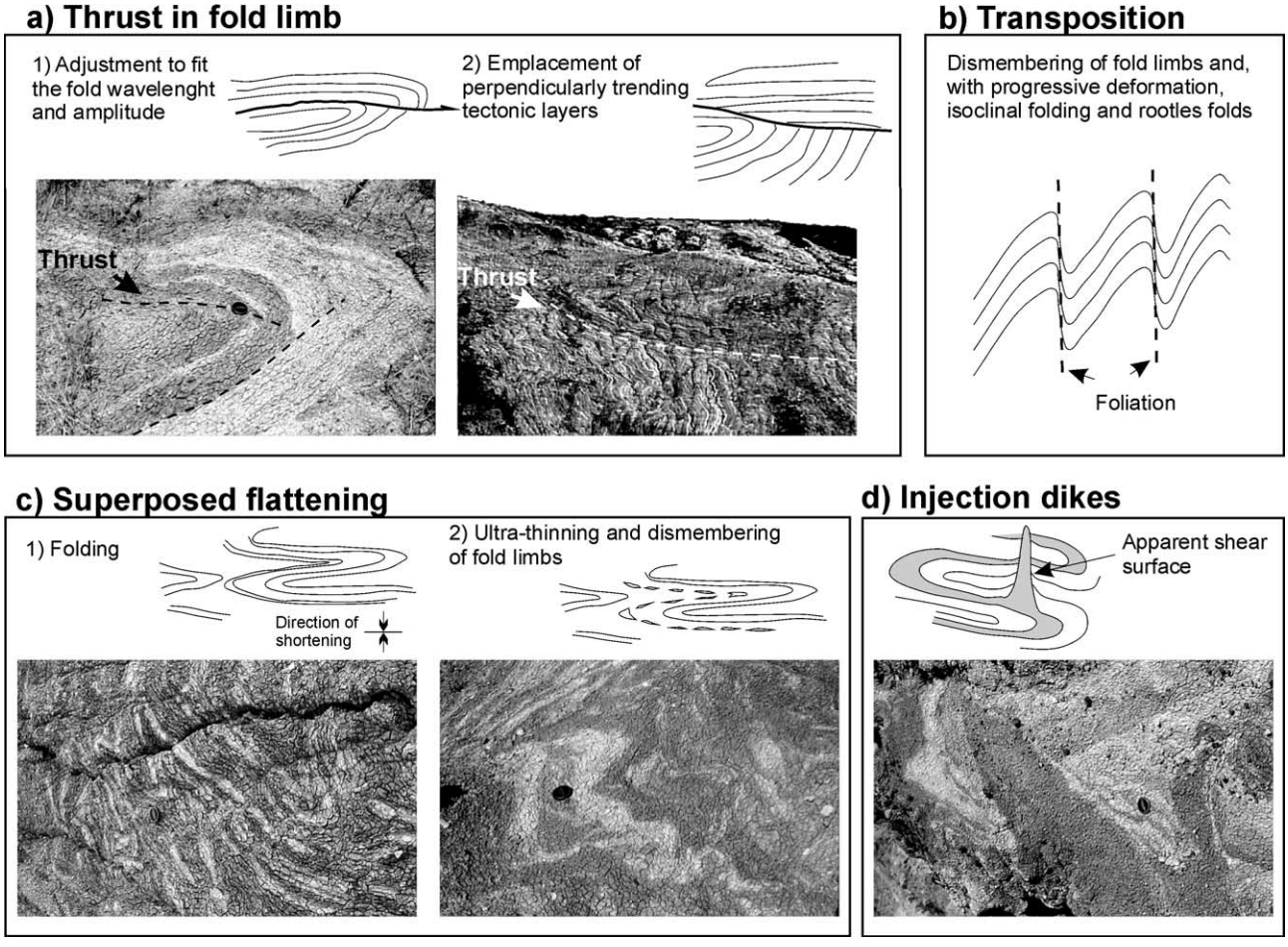

Fig. 9. True and apparent shear surfaces in Multilayer 3 with mechanisms of formation as recognized in the field.

other at very low angle, give a distinctive anastomosing pattern comparable with a tectonic cross-stratification (Fig. 8a). These shear surfaces maintain the cohesion of the shaly mass, in fact they cause the rock to split in long and narrow bodies of various sizes with tabular, lozenge or lenticular shape. At the outcrop scale their long axes are markedly sub-parallel to each other producing a striking planar tectonic layering, S_1 (Fig. 5g). S_1 is a mappable feature and is typically very gently dipping since it is parallel or sub-parallel to the basal contact with the overlying epi-Ligurian sequence, where preserved.

The S_1 surfaces bound very deformed shaly volumes characterized by penetrative scaly fabric at the scale of the sample. The scaly fabric can be either parallel or sub-parallel to the bounding mesoscopic shear surfaces. The original S_0 layers of alternating varicolored shales appear stretched, thinned, discontinuous or as irregular strips and bands parallel to the scaly fabric.

The rare competent layers, usually gray marls, occur as very irregular inclusions of various shape, usually spheroid or egg-like shapes. Within the deformed volumes defined by the S_1 surfaces, there are portions with segments of a single layer or packages of layers still stratigraphically ordered. Such cases are very rare since usually the most common features in the S_1-defined volumes are stratal disruption, and irregular to isoclinal rootless folds.

The geometric relationship between coherent and incoherent units is often difficult to establish. Where the contact is directly detectable in the field it develops in several different ways. It can be transitional or the coherent units may be found completely surrounded by incoherent ones and vice versa. In folded sequences, the contact often occurs through a marked shear surface that lies at high angle to the limbs and axial surfaces of the folds; the shear surface may also cut some of the folds.

6.1.1. Boudinage and pinch-and-swell structures

The rare limestone, calcareous marl, sandstone and micro-conglomerate layers are everywhere laterally discontinuous and reduced to isolated blocks. Although the blocks are isolated, the colors of the surrounding shaly layers help to show the geometry of the deformation and to link them together.

The calcareous blocks are internally deformed by brittle structures as extension fractures with blocky or fibrous calcite veins and extensional shear fractures. These features, which resemble those in Multilayer 1, show that the boudinage of competent layers was achieved by extension parallel to S_0. The extension developed when the beds were already completely lithified and occurred along two almost perpendicular and non-contemporaneous directions. Sandstone and micro-conglomerate boudins show structures that reveal the same deformational regime as the calcareous blocks, but under pre-lithification conditions as in Multilayer 2, showing that deformation occurs through hydroplastic shear fractures and grain-boundary sliding.

6.1.2. Folds

The coherent and the disrupted portions of Multilayer 3 are systematically characterized by complex mesoscopic folds, with a variety of styles depending on the prevailing lithotype as well as the thickness of the folded beds (Fig. 8), and by shear surfaces (Fig. 9). At the same outcrop tight-to-isoclinal similar folds, chevron folds with various interlimb angles and disharmonic to convolute folds occur next to each other. Chevron folds are predominantly developed in thinly bedded shales with thin scattered sandstone–siltstone layers, while disharmonic and convolute folds typically develop in the black or red-purple shales.

Two systems of folds with perpendicular hinge-lines characterize also this multilayer (Fig. 5h) and refolded folds are frequent. Usually the two folds have different dimensions and tightness, but in some cases type 2 interference patterns were clearly observed at the outcrop scale. Small scale superimposed perpendicular folds affecting single sandstone layers are common in sequences of alternating thin-bedded sandstones and shales (Fig. 8). In this case tight-to-isoclinal folds with a sub-horizontal axial surface usually represent the first generation of folds, whereas the folds of the second generation are open with a vertical axial surface and a sub-horizontal hinge line. The limbs of the close-to-isoclinal folds are affected by an intense boudinage of brittle, semibrittle or ductile type, or in the form of pinch-and-swell structures according to the lithotypes and to their competence contrast (Fig. 8c). Bulbous hinges and secondary features such as thrusts, either singly or in conjugate pairs, are frequent as structures formed to accommodate the thickness difference of the folded beds. Very common is also the over-thickening of the shaly beds, particularly the black and red, in the hinges of the similar folds. In this case the hinge zone developed either a marked scaly fabric forming a divergent fan toward the intrados of the fold, or small folds refolding both the primary fissility and the scaly fabric. A prominent scaly fabric sub-parallel to S_0 is also present on the limbs of the folds, at the layer interfaces, either with or without limb thrusts. Locally the coherent units present zones where the deformation style is characterized by convolute and disharmonic folds, rootless folds and isolated fold hinges associated with an intense boudinage leading to a loss of the lateral continuity of the layers. A penetrative scaly fabric, which according to the segments of still recognizable bedding is parallel to S_0, marks the folds. These zones of intense deformation are generally restricted to the red and black shales with sparse thin beds of gray to white marlstones, and are typically characterized by undefined boundaries. Frequently sharp mesoscopic shear surfaces intersect the folded units and place in contact folded volumes with different attitude and/or style of deformation. These shear surfaces are clearly sealed by the overlying epi-Ligurian sequence and they have a distinctive morphology that differs from the brittle faults generated by younger tectonic phases. In fact, while the cohesion of the rock is maintained, a

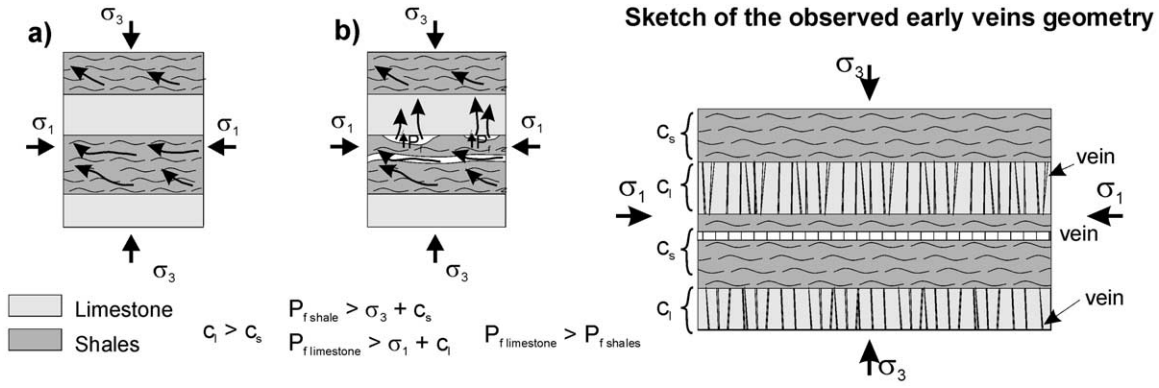

Fig. 10. Diagram of the hydrologic regime as interpreted from the structural analysis.

penetrative scaly fabric is developed parallel to the shear surface for a thickness of few millimeters to some centimeters.

Locally cores of isoclinal folds developed in the red shales are shot through forming diapiric and extrusion structures in the hinge zones and/or in the limbs of the folds (Fig. 9d). The injection dykes, centimeters to some meters long, usually cut the fold limbs and the cohesive shear surfaces just described. These injection dykes are filled by the same shaly material as the host rock and are characterized by a penetrative scaly fabric. All these structures clearly suggest that at least some of the pelitic horizons, although already largely deformed by folds and faults, still maintained a very high ductility and a large amount of fluids.

The folds in Multilayer 3 are cut and dismembered by shear surfaces (Fig. 9). Diapiric structures and injection dykes, testifying that the shales were still fluid-rich and not yet completely lithified, cross-cut these shear surfaces, which are often the most evident mesoscopic structures in Multilayer 3 outcrops (Fig. 8a). These cohesive surfaces are few meters to some hectometers long and cross-cut each other at low angles splitting the Multilayer 3 in blocks of various shape where rootless folds, boudinage and pinch-and-swell are present. Thus incoherent units mainly derive from a further deformation of the coherent units since they preserve relicts of their early deformation history.

7. Structural evolution of the multilayers

7.1. Pre-folding events

The structural evolution records the changes in mechanical properties that accompany compaction and lithification. The primary fissility, still undeformed in coherent multilayers or in the fold hinges, is the result of the initial compaction. Compaction and lithification are associated with fluid expulsion and, in fact, the first deformation event recorded by Multilayer 1 is the development of thin veins (Fig. 4) and fibrous calcite veins parallel to S_0, with the fibers normal to S_0 (Fig. 6b). The latter are only in the shaly layers or at the interface between limestone and shaly beds and they are folded by the two events and boudinaged as the sedimentary limestone-rich component of Multilayer 1, suggesting they were formed when the multilayer was still coherent (Fig. 10). Flow structures in the boudin neck region imply the shales were not already lithified, even though, as the fractures testify, they locally had some strength (Vannucchi and Maltman, 2000). Thin veins, filled by syntaxial dirty calcite, cut only the limestone-rich component of Multilayer 1. Since thin veins do not show geometrical relationships either with folds or boudins, they are assumed to be pre-folding. Thin veins indicate that the limestone-rich layers were already able to fracture and the style of deformation was typically brittle.

The two vein systems never intersect, since the veins parallel to S_0 are only associated with the shales, while the thin veins are from only within the limestone-rich layers (Fig. 10). On the other hand, both vein systems testify to fluid expulsion during the early stages of deformation. Based on the geometric assessment and the microscopic characters of the mineralization, in fact, they have been attributed to fluid overpressure and hydraulic fracturing (Maltman, 1994; Vannucchi and Maltman, 2000). Besides, these early deformation features suggest a different degree of lithification reached inside Multilayer 1, with the limestone-rich component having undergone lithification prior to folding, while the shaly layers were still able to flow. The heterogeneous lithification implies that the average cohesion of the shales, c_s, was lower than the cohesion of the limestone-rich layers, c_l (Fig. 10). This difference of cohesion implies that the shales could fracture under a lower fluid pressure. Heterogeneous lithification caused fluid circulation inside Multilayer 1 to be characterized by shale dewatering, and limestone-rich layers acting as an obstruction (Fig. 10a). Dewatering fluid will thus accumulate at the base of the limestone-rich layers generating high fluid pressure until fracturing is induced (Fig. 10b). This mechanism can also explain why in the early phases of deformation veins parallel to S_0 only characterize both Multilayers 2 and 3. In the case of Multilayer 2, in fact, the fluid pressure could not build up at the base of the

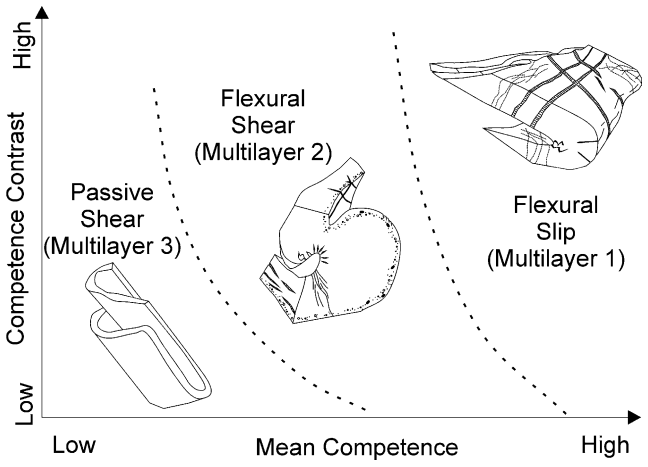

Fig. 11. Multilayer folding mechanisms depending on the mean competence of the whole multilayer and the contrast in competence among individual layers.

siliciclastic layers, since they were not yet lithified at this time of deformation, and very permeable. In the case of Multilayer 3 the difference between the physical properties of the alternating material was not relevant.

7.2. Folding events

The deformation goes on in the three multilayers with the development of non-cylindrical isoclinal folds accompanied by the formation of extensional fractures perpendicular to S_0 in the already lithified components. The heterogeneous lithification and the progressive hardening of the multilayers as the deformation proceeds is testified to by the gradual appearance of structures related to the folding as the axial plane cleavage.

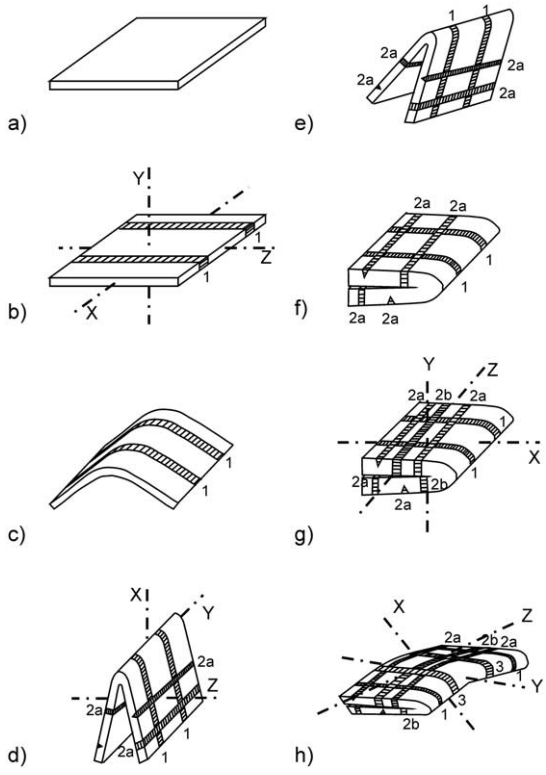

Fig. 12. Diagram of the fold-related vein development as interpreted from the structural analysis.

To describe the effect of folding in the multilayered sequences it is necessary to analyze the competence contrast among individual layers and the competent/incompetent layer ratio among the multilayers and even within each multilayer (Fig. 11). Locally, in fact, the multilayers can have a coherent or incoherent appearance, and this is the effect of increasing the ratio of incompetent shale to competent material, limestone-rich or sandstone layers. Starting with Multilayer 1 a common character of the fold hinges is the shortening in the concave side and the stretching in the convex side of each competent layer. Thus, across a bedding surface, the layer records a relative slip typical of flexural slip folding (Fig. 11). Depending on the competence contrast, the shear can be concentrated along the layer interfaces, or can be uniformly distributed across the incompetent layers. If the shaly layers are thicker than the limestone-rich ones, the potential slip between competent layers will be taken up by shear within the shales, still unlithified at the time of folding. The shear across the shaly layers produces slippage at the level of clay particles. This situation agrees with the scaly fabric occurrence. The relative importance between differential slip among competent and soft layers, limb thinning and clay particle collapse due to an instantaneous decrease in fluid overpressure (Vannucchi and Maltman, 2000) in the scaly fabric development is the object of further analysis not reported in this paper.

Typically the described folds have thickened hinges, class 1C, class 2 or class 3 folds, and boudinaged limbs. Folds and boudins appear to have formed together and the boudin necks are parallel to the fold hinges. Such a relationship can be associated with the sequential development of folds and boudins during a single deformation event since the folding layers pass from regions of contraction to regions of extension (Price and Cosgrove, 1990). This effect is also further amplified by the high competence contrast within Multilayer 1. The folds in all the analyzed multilayers show sub-horizontal axial planes and this argues for a progressive noncoaxial deformation (i.e. simple shear).

The most important minor structures created during folding are the extensional calcite veins. The oldest veins (1 in Fig. 12), with fibers parallel both to S_0 and to the F_1 hinge line, are folded by F_1. This geometry implies that the first veining event is associated with the volume adjustment subsequent to the shortening in the *Z* direction during buckling, responsible for folds with axes parallel to *X*. In this case, in fact, the layer may develop extension parallel to *X* (Price and Cosgrove, 1990) (Fig. 12b). The progressive folding mechanism causes further deformation of this first group of veins (Fig. 12c) and the development of a second fold-related veining event (Fig. 12d). The second veining event (2a in Fig. 12), with fibers perpendicular to the F_1

hinge line, is associated with the stretching of the competent layer on the limb of a developing fold as an effect of the rotation into the extension field as the fold amplifies (Fig. 12d). The same mechanism is responsible for the extensional fractures and the extensional shear fractures resulting in the symmetrical or asymmetrical boudinage of the strong beds involved in the fold limbs. The first folding event ended with the progressive closure of the fold, which becomes isoclinal, and the contemporaneous rotation of the axial plane, which becomes horizontal (Fig. 12e).

The second folding event produced close to isoclinal folds with axes and axial planes sub-perpendicular to F_1. Except for the different orientation and for a stronger behavior of the multilayer components, as a consequence of a higher degree of lithification, the same features described for F_1 characterizes F_2. The competence contrast and the competent/incompetent ratio are the major parameters controlling the folding mechanism. This new stress field, with maximum compressive stress perpendicular to the first one, causes the deformation of all the previously formed structures like joints, extensional veins and extensional shear fractures, and the development of new features. In particular the second folding event produces new veining (2b in Fig. 12). These extensional veins developed parallel to the maximum principal stress along the *Z* axes and have the fibers parallel to F_2 hinge line (Fig. 12g). The geometry of 2a and 2b veins (refer to Fig. 12) is basically the same and they do not have a distinctive time relationship. The clear existence of two groups of veins related to different folding events has been proven by field observations on cross-cutting relationships among the secondary, refolded features. This model also satisfies the symmetry relationship between folds and related veins. The stretching of the limbs of F_2 folds (Fig. 12h) generates the last veining event (3 in Fig. 12). The extensional vein geometry gives evidence of two perpendicular directions of extension directly linked to the superposition of two perpendicular fold generations.

Multilayers 2 and 3 are characterized by a lower competence contrast than Multilayer 1, but they resemble the same structural evolution. The fabric data of Multilayer 2 show a greater dispersion than in Multilayer 1, because of the lack, or the incomplete development, of a well-defined tectonic foliation. This dispersion is caused by the presence of chevron and open folds, which prevent the complete transposition of the primary bedding. The sandstone layers in Multilayer 2 were not lithified at the time of the first folding event at least and it can be described having a moderate mean competence and moderate competence contrast. In this case the potential slip between the layers is taken up by shear within layers (Fig. 11). The effect on the shaly material is similar to what has been described for Multilayer 1, while the sandy–silty layers deform through particulate flow (Maltman, 1994), so that virtually no traces of the shear associated with folding has been left in these layers. The high amount of fluids trapped in the sandy–silty layers is also indicated by the presence of veins in the inner arc of the fold hinges, as fluids escape tracks. The high fluid pressure originated by the effect of the wrapping shales on the sandy–silty layers locally determines softening and dilation of the sediments producing arrays of sediment-filled veins. The folding mechanism can be referred to as flexural flow (Fig. 11).

Multilayer 3 has a low mean competence and a low competence contrast (Fig. 11). The high fluid content is partly due to the very low permeability, which prevented compaction and fluid expulsion, but also Multilayer 3 is the youngest unit of the sequence and it was deformed in the early stage of the diagenetic process. Interfaces are defined within the multilayer by sedimentary surfaces, but the material can be considered mechanically homogeneous. The layers have a minimum slip and they rather behave as passive markers of the deformation. The folding mechanism is referred to as passive shear with homogeneous flattening (Fig. 11). Boudins and extensional shear fractures are sparse in Multilayer 3 suggesting that locally strain hardening played an important role. The widespread shear surfaces developed during the late stages of folding when the shales were not fully lithified, as demonstrated by the intersection of diapiric structures and injection dykes. Their geometry and morphology suggest they were formed by thrust in the fold limbs, flattening and transposition of the folded multilayers and also by diapiric events. All these mechanisms are well documented in the field (Fig. 9). These shear surfaces, responsible for the highly disrupted exposure of Multilayer 3, are connected to folding mechanisms.

8. Conclusions

The recognition that the internal structure of a mélange is not chaotic so that it can be studied using the techniques applied to deeper levels of the crust is not new (Needham, 1995; Vannucchi and Maltman, 2000), and the systematic study to reconstruct the geometry and the tectonic mechanism which disrupts the Apennine tectonic mélanges has been a matter of debate for many years now (Castellarin et al., 1986; Bettelli and Panini, 1989; Castellarin and Pini, 1989; Pini, 1999). This study contributes to this discussion and represents the first effort to develop a consistent geometric frame to the internal geometry of the Apennine tectonic mélanges.

The Apennine tectonic mélanges exhibit folding remnants and disruption that occurred through two perpendicular directions of layer-parallel extension. This occurrence is not rare in broken formations and, in fact, has been reported by several authors, each one giving a different indication of possible formation (Cowan, 1990; Holdsworth and Grant, 1990; Needham, 1995). While the layer parallel extension in two perpendicular directions is, in fact, well explained for the sedimentary mélanges deformed in a near surface environment through a mechanism of lateral spreading inducing flattening as effect of mass wasting (Brandon,

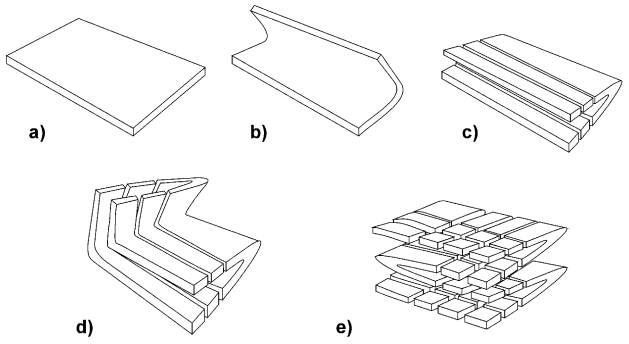

Fig. 13. Diagram of the internal geometry responsible for the chaotic aspect of the multilayers. Steps (a)–(e) show the development of progressive disruption of the rock as effect of two perpendicular folding phases with limb stretching.

1989; Cowan, 1990), the tectonic mechanisms are still a matter of debate. The widespread occurrence of layer-parallel extension and the evidence it occurs during the accretion, so that the characteristic oblate blocks form, force the authors to assume a sufficient amount of lateral spreading in accretionary prisms. Among the possible causes of this spreading, a taper angle change can induce a flattening component across the basal shear-zone of an accretionary prism (Davis et al., 1983; Waldron et al., 1988). The same taper angle change causing shortening, on the other hand, may bring the development of out-of-sequence thrusts forming a broad shear-zone through steeply dipping beds which are favorably oriented to undergo extension during progressive shear. The changes in plate convergence vector and oblique subduction are also mechanisms that cause stretching, although small, as illustrated by McCaffrey et al. (2000) (cum bibl.). Study of deformation in deeper level settings suggests that flattening can occur across a basal shear zone to a thrust sheet, the 'dynamic spreading' (Holdsworth and Grant, 1990). This mechanism implies bulk viscous rheology and major thrusts separating sheets where the strain increases approaching the detachment zone allowing the perpendicular layer parallel extension (Needham, 1995). All these mechanisms lead to the development of extensional structures, but the flattening component is confined to the basal shear zone of accretionary prisms, to orogen-parallel strike-slip faulting or to major thrusts. Since the Apennine mélanges involve the entire basal portion of the External Ligurian Units (700–800 m thick) and thrusts are minor features, these mechanisms appear inappropriate for the Ligurian mélanges. Besides the classical extensional models challenge the widespread development of folds and their perpendicular refolding. In fact, early folds have been reported from mélanges, as for example the McHugh Complex (Kusky et al., 1997), but they have been related to post-disruption rotations.

The detailed analysis of the Apennine tectonic mélanges and their geometry support a mechanism where folding, i.e. shortening, drives perpendicular layer parallel extension. This mechanism acted throughout the basal portion of the External Ligurian Units since the three examined multilayers exhibit different physical properties and degree of disruption, but they match the same structural evolution. The structures collected in the multilayers are bearing witness to, in fact, the superposition of two generations of perpendicular folds (Fig. 13) causing two perpendicular, not-coeval directions of layer parallel extension. The degree of disruption is the result of the competence contrast and the competent/incompetent ratio, so that the wide variety of mélange structures is mainly controlled by mechanical factors acting in the same geodynamic environment. The latter is here constrained by the slope apron sequences, epi-Ligurian, resting on top of the described units and the lack of an appreciable metamorphism of these units. The epi-Ligurian sequence unconformably overlies the studied sequences and testifies that these latter have been deformed before the middle Eocene. Thus, in the general frame defined by the Ligurian convergence, the described multilayers have been disrupted at superficial levels of the crust during or in the phases near to the frontal accretion before the collision between the European and Adria plates. The occurrence of layer-parallel extension as a result of repeated folding leads to shortening as the controlling mechanism, in agreement with the recognition that deformation took place simultaneously with the frontal accretion.

The model described in Fig. 12 can be applied in other sectors of the same chain, such as the Sicilian Units of the Southern Apennines where similar features have been described (Roure et al., 1991), and even to other parts of the world, since it is only based on the physical properties of the deforming material. Regarding the genesis of the described deformation geometry the study is the subject of a paper in preparation. The superposition of two generations of perpendicular folds, in fact, may be either the result of the particular tectonic configuration where the Ligurian convergence occurred, or may be a common deformation style of the sediments entering a subduction complex.

Acknowledgements

We thank our colleagues Marco Capitani and Filippo Panini for the stimulating discussions in the field. Darrel Cowan provided a critical review that helped clarify our presentation. Reviews by Gian Andrea Pini, Mark Brandon and the editor Richard Lisle greatly improved the manuscript.

References

Abbate, E., Sagri, M., 1970. The eugeosynclinal sequences. In: Sestini, G. (Ed.), Development of the Northern Apennines Geosyncline. Sedimentary Geology 4, pp. 521–557.

Bettelli, G., Panini, F., 1989. I mélanges dell'Appennino Settentrionale dal T. Tresinaro al T. Sillaro. Memorie della Società Geologica Italiana 39, 187–214.

Bettelli, G., Panini, F., 1992. Liguridi, mélanges e tettoniti nel complesso caotico lungo la "linea del Sillaro" (Appennino Settentrionale,

Provincie di Firenze e Bologna). Memorie Descrittive della Carta Geologica d'Italia 46, 387–415.

Bettelli, G., Bonazzi, U., Panini, P., 1989a. Schema introduttivo alla geologia delle Liguridi dell'Appennino modenese e delle aree limitrofe. Memorie della Società Geologica Italiana 39, 91–125.

Bettelli, G., Bonazzi, U., Fazzini, P., Panini, F., 1989b. Schema introduttivo alla geologia delle Epiliguridi dell'Appennino Modenese e delle aree limitrofe. Memorie della Società Geologica Italiana 39, 215–244.

Bettelli, G., Capitani, M., Panini, F., Pizziolo, M., 1996. Le rocce caotiche dell'Appennino emiliano: metodi sperimentali di rilevamento stratigrafico, esempi e nomenclatura. Accademia Nazionale di Scienze, Lettere ed Arti di Modena, Collana di Studi 15, 189–220.

Boccaletti, M., Coli, M., Decandia, F., Giannini, E., Lazzarotto, A., 1980. Evoluzione dell'Appennino Settentrionale secondo un nuovo modello strutturale. Memorie della Società Geologica Italiana 21, 359–373.

Brandon, M.T., 1989. Deformational styles in a sequence of olistostromal mélanges, Pacific Rim Complex, western Vancouver Island, Canada. Geological Society of America Bulletin 101, 1520–1542.

Byrne, T., 1984. Early deformation in mélange terranes of the Ghost Rocks Formation, Kodiak Islands, Alaska. In: Raymond L.A. (Ed.), Mélanges: their Nature, Origin, and Significance. Geological Society of America, Special Paper 198, pp. 21–51.

Byrne, T., Fisher, D., 1990. Evidence for a weak and overpressured décollement beneath sediment-dominated accretionary prisms. Journal of Geophysical Research 95, 9081–9097.

Capedri, S., Toscani, L., 2000. Subduction-related ophiolitic metabasalts from Northern Apennines (Modena Province, Italy). Chemie der Erde—Geochemistry 60, 111–128.

Castellarin, A., Pini, G.A., 1989. L'arco del Sillaro: la messa in posto delle Argille Scagliose al margine appenninico padano (Appennino bolognese). Memorie della Società Geologica Italiana 39, 127–141.

Castellarin, A., Pini, G.A., Crestana, G., Rabbi, E., 1986. Caratteri strutturali mesoscopici delle Argille Scagliose dell'Appennino bolognese. Memorie di Scienze Geologiche 38, 459–477.

Charvet, J., Ogawa, Y., 1994. Arch-trench tectonics. In: Hancock, P.L. (Ed.). Continental Deformation. Pergamon Press, Oxford, pp. 180–199.

Clennell, M.B., Maltman, A.J., 1995. Microstructures in accreted sediments of the Cascadia Margin. In: Carson, B., Westbrook, G.K., Musgrave, R.J., Suess E. (Eds.), Proceedings of the Ocean Drilling Program, Scientific Results 146, pp. 201–216.

Cowan, D.S., 1985. Structural styles in Mesozoic and Cenozoic mélanges in the western Cordillera of North America. Geological Society of America Bulletin 96, 451–462.

Cowan, D.S., 1990. Kinematic analysis of shear zones in sandstone and mudstone of the Shimanto Belt, Shikoku, SW Japan. Journal of Structural Geology 12, 431–441.

Coward, M., Dietrich, D., 1989. Alpine tectonics—an overview. In: Coward, M., Dietrich, D. (Eds.), Alpine Tectonics, Geological Society Special Publication 45, pp. 1–29.

Davis, D.M., Suppe, J., Dahlen, F.A., 1983. Mechanics of fold and thrust belts and accretionary wedges. Journal of Geophysical Research 88, 1153–1172.

Deiana, G., Pialli, G., 1994. The structural provinces of the Umbro–Marchean Apennines. Memorie della Società Geologica Italiana 48, 473–484.

De Nardo, M.T., 1994. "Chaotic units" outcropping between the Termina di Castione and Tassobbio valleys (Parma and Reggio Emilia Apennines). Memorie della Società Geologica Italiana 48, 295–299.

Fisher, D., Byrne, T., 1987. Structural evolution of underthrusted sediments, Kodiak Islands, Alaska. Tectonics 6, 775–793.

Fruehn, J., Von Huene, R., Fisher, M.A., 1999. Accretion in the wake of terrane collision: the Neogene accretionary wedge off Kenai Peninsula, Alaska. Tectonics 18, 263–277.

Harris, R.A., Sawyer, R.K., Audley-Charles, M.G., 1998. Collisional mélange development: geologic associations of active mélange-forming processes with exhumed mélange facies in the western Banda orogen, Indonesia. Tectonics 17, 458–479.

Hashimoto, Y., Kimura, G., 1999. Underplating process from mélange formation to duplexing: example from the Cretaceous Shimanto Belt, Kii Peninsula, southwest Japan. Tectonics 18, 92–107.

Holdsworth, R.E., Grant, C.J., 1990. Convergence related dynamic spreading in a mid-crustal ductile thrust zone: a possible orogenic wedge model. In: Knipe R.J., Rutter, E.H. (Eds.), Deformation Mechanisms, Rheology and Tectonics, Special Publication of the Geological Society of London 54, pp. 491–500.

Hsü, K., 1968. Principles of mélanges and their bearing on the Franciscan–Knoxville paradox. Geological Society of America Bulletin 79, 1063–1074.

Kimura, G., Mukai, A., 1991. Underplated units in an accretionary complex: mélanges of the Shimanto Belt of Eastern Shikoku, Southwest Japan. Tectonics 10, 31–50.

Kusky, T.M., Bradley, D.C., 1999. Kinematic analysis of mélange fabrics: examples and applications from the McHugh Complex, Kenai Peninsula, Alaska. Journal of Structural Geology 21, 1773–1796.

Kusky, T.M., Bradley, D.C., Haeussler, P.J., Karl, S., 1997. Controls on accretion of flysch and mélange belts at convergent margins, evidence from the Chugach Bay thrust and Iceworm mélange, Chugach accretionary wedge, Alaska. Tectonics 16, 855–878.

Lewis, J.C., Byrne, T., 1996. Deformation and diagenesis in an ancient mud diapir, southwest Japan. Geology 24, 303–306.

Maltman, A.J., 1994. Prelithification deformation. In: Hancock, P.L. (Ed.). Continental Deformation. Pergamon Press, Oxford, pp. 143–158.

Maltman, A.J. (Ed.), 1995. The Geological Deformation of Sediments. Chapman and Hall, London.

Maltman, A.J., Byrne, T., Karig, D.E., Lallemant, S., 1993. Deformation at the toe of an active accretionary prism: synopsis of results from ODP Leg 131, Nankai, SW Japan. Journal of Structural Geology 15, 949–964.

Marroni, M., 1994. Deformation path of the internal Ligurid Units (Northern Apennines, Italy): record of shallow-level underplating in the Alpine accretionary wedge. Memorie della Società Geologica Italiana 48, 179–194.

Marroni, M., Pandolfi, L., 1996. The deformation history of an accreted ophiolite sequence: the internal Liguride units (Northern Apennines, Italy). Geodinamica Acta 9, 13–29.

Marroni, M., Treves, B., 1998. Hidden terranes in the Northern Apennines, Italy: a record of Late Cretaceous–Oligocene transpressional tectonics. Journal of Geology 106, 149–162.

McCaffrey, R., Zwick, P.C., Bock, Y., et al., 2000. Strain partitioning during oblique plate convergence in northern Sumatra: Geodetic and seismologic constraints and numerical modeling. Journal of Geophysical Research 105, 28363–28376.

Merla, G., 1952. Geologia dell'Appennino Settentrionale. Bollettino della Società Geologica Italiana 70, 95–382.

Needham, D.T., 1995. Mechanisms of mélange formation: examples from SW Japan and southern Scotland. Journal of Structural Geology 17, 971–985.

Orange, D.L., 1990. Criteria helpful in recognizing shear-zone and diapiric mélanges: examples from the Hoh accretionary complex, Olympic Peninsula, Washington. Geological Society of America Bulletin 102, 935–951.

Page, B.M., 1963. Gravity tectonics near Passo della Cisa, Northern Apennines, Italy. Geological Society of America Bulletin 74, 655–672.

Pini, G.A., 1992. Associazioni micro-mesostruttturali nelle Argille Scagliose (pedeappennino bolognese): loro significato genetico. Memorie Descrittive della Carta Geologica d'Italia 4, 355–373.

Pini, G.A., 1999. Tectosomes and Olistostromes in the Argille Scagliose of the Northern Apennines, Italy. Geological Society of America Special Paper 335, 70pp.

Price, N.J., Cosgrove, J.W., 1990. Analysis of Geological Structures. Cambridge University Press, Cambridge.

Principi, G., Treves, B., 1984. Il sistema Corso-Appenninico come prisma d'accrezione. Riflessi sul problema generale del limite Alpi-Appennini. Memorie della Società Geologica Italiana 28, 549–576.

Ramsay, J.G., Huber, M.I., 1987. The Techniques of Modern Structural Geology, Volume 2: Folds and Fractures. Academic Press, London.

Raymond, L.A., 1984. Classification of mélange. In: Raymond L.A. (Ed.), Mélange: their Nature, Origin, and Significance, Geological Society of America, Special Paper 198, pp. 7–20.

Reutter, K.J., 1981. A trench-forearc model for the Northern Apennines. In: Wezel, F.C. (Ed.). Sedimentary Basins of Mediterranean Margins. C.N.R. Italian Project of Oceanography. Tecnoprint, Bologna, pp. 433–443.

Ricci Lucchi, F., 1987. Semi-allochthonous sedimentation in the Apennine Thrust-Belt. Sedimentary Geology 50, 119–134.

Roure, F., Casero, P., Vially, R., 1991. Growth-processes and mélange formation in the southern Apennines accretionary wedge. Earth and Planetary Science Letters 102, 395–412.

Treves, B., 1984. Orogenic belts as accretionary prisms: the example of the Northern Apennines. Ofioliti 9/3, 577–618.

Vai, G.B., Castellarin, A., 1993. Correlazione sinottica delle unità stratigrafiche nell'Appennino Settentrionale. In: Capozzi, R., Castellarin, A. (Eds.), Studi preliminari all'acquisizione dati del profilo CROP1-1A La Spezia-Alpi orientali. Studi Geologici Camerti, Volume Speciale 1992/2, pp. 171–185.

Vannucchi, P., Maltman, A.J., 2000. Insights into shallow-level processes of mountain building from the Northern Apennines, Italy. Journal of the Geological Society, London 157, 105–120.

Vescovi, P., Fornaciari, E., Rio, D., Valloni, R., 1999. The Basal Complex Stratigraphy of the Helminthoid Monte Cassio Flysch: a key to the Eoalpine tectonics of the Northern Apennines. Rivista Italiana di Paleontologia e Stratigrafia 105 (1), 101–128.

Vollmer, F.W., Bosworth, W., 1984. Formation of mélange in a foreland basin overthrust setting: example from the Taconic Orogen. In: Raymond L.A. (Ed.), Mélange: their Nature, Origin, and Significance, Geological Society of America, Special Paper 198, pp. 53–70.

Waldron, J.F., Turner, D., Stevens, K.M., 1988. Stratal disruption and development of mélange, western Newfoundland: effect of high fluid pressure in an accretionary terrain during ophiolite emplacement. Journal of Structural Geology 10, 861–873.